Vortex Mutual Friction, Orbital Inertia, and History-Dependent Textures in Rotating Superfluid ^{3}He-*A*

A. J. Manninen,* T. D. C. Bevan, J. B. Cook, H. Alles, J. R. Hook, and H. E. Hall
Schuster Laboratory, University of Manchester, Manchester, M13 9PL, United Kingdom
(Received 16 September 1996)

We have measured the resistive and reactive mutual friction coefficients in rotating superfluid ^{3}He-*A* at 29.3 bars pressure. The results agree with those predicted from the equation of orbital hydrodynamics for two quantum continuous vortices if the previously measured value of the orbital viscosity is used. Our results put an upper limit on the orbital inertia of less than $0.005\hbar$ per Cooper pair. We explain our observation of history-dependent textures by noting that the ease of formation of continuous vortices depends on the relative direction of $\mathbf{l}$ and the rotation axis. [S0031-9007(96)01886-8]

PACS numbers: 67.57.Fg, 47.37.+q, 67.57.De

In superfluid ^{3}He-*A* rotating at a small angular velocity Ω in a small magnetic field it is expected that nonsingular dipole-locked continuous vortices will be created [1] to allow the superfluid to simulate solid body rotation. An interesting property of such vortices is that the mutual friction they produce should be fully determined by two macroscopic hydrodynamic coefficients, the orbital viscosity, and the orbital inertia [2], which enter the equation of motion of the orbital vector $\mathbf{l}$. Mutual friction measurements thus provide a good method for measuring the orbital inertia; the magnitude of this and its relationship to "intrinsic angular momentum" has been a subject of some controversy [3]. In this Letter we present mutual friction measurements that enable us to put an upper limit on the orbital inertia of $0.005\hbar$ per Cooper pair; this is significantly smaller than can be achieved, for example, in orbital relaxation measurements [4]. Our result favors microscopic calculations which predict a magnitude of order $(k_B T_C/\epsilon_F)^2\hbar$ per Cooper pair [5]. The measured resistive component of mutual friction agrees with that predicted using previously measured values of the orbital viscosity [4].

To make reliable mutual friction measurements we had to develop a method for obtaining a uniform $\mathbf{l}$ texture in the nonrotating state. We discovered that the best way of achieving this was to cool through T_C while rotating in a magnetic field smaller than the Freedericksz transition field [6]. We were at first surprised to find that the liquid *remembered* the sense of rotation used during this initial cooldown in that after a further rotation in the same direction the uniform texture was reestablished, but following a rotation in the opposite sense a nonuniform texture was obtained. After presenting the mutual friction data we give more details of this textural memory effect and present a simple explanation, based upon the realization that the initial sense of rotation determines the direction of the uniform $\mathbf{l}$ texture.

In rotating equilibrium vortices give rise to a mutual friction force

$$\mathbf{F}_{ns} = 2\alpha\rho_{s\perp}\Omega(\mathbf{v}_s - \mathbf{v}_n)_\perp - 2\alpha'\rho_{s\perp}\mathbf{\Omega}\times(\mathbf{v}_s - \mathbf{v}_n) \tag{1}$$

per unit volume between the normal and superfluid components, where $\rho_{s\perp}$ is the superfluid density for flow perpendicular to $\mathbf{l}$ and the dimensionless parameters α and α' give, respectively, the magnitudes of the resistive (longitudinal) and reactive (transverse) components of the force. Our notation is consistent with that of [7]; we use α and α' rather than the more usual B ($\equiv 2\rho\alpha/\rho_{n\perp}$) and B' ($\equiv 2\rho\alpha'/\rho_{n\perp}$) because it is the former that are directly measured in our experiment. Theories usually calculate dimensional quantities D and D' that characterize the force acting on unit length of vortex line because of its motion relative to the normal fluid. The force balance equation for a vortex moving at velocity $\mathbf{v}_L$ is written

$$\rho_{s\perp}\kappa\hat{\mathbf{z}}\times(\mathbf{v}_L - \mathbf{v}_s) = D(\mathbf{v}_L - \mathbf{v}_n) + D'\hat{\mathbf{z}}\times(\mathbf{v}_L - \mathbf{v}_n), \tag{2}$$

where the left-hand side is the Magnus force resulting from relative motion of the vortex and superfluid. The dimensionless forms of D and D', given by $d_\parallel = D/\rho_{s\perp}\kappa$ and $d_\perp = D'/\rho_{s\perp}\kappa$, are related to α and α' by

$$d_\parallel = \frac{\alpha}{\alpha^2 + (\alpha' - 1)^2}, \tag{3}$$

$$d_\perp - 1 = \frac{\alpha' - 1}{\alpha^2 + (\alpha' - 1)^2}. \tag{4}$$

If the length scale of the vortices is long compared to the excitation mean free path and the mutual friction force is assumed to arise from the motion of undistorted continuous vortices, then the mutual friction force can be calculated [2] from the orbital hydrodynamic equation

$$-\lambda\mathbf{l}\times\frac{d\mathbf{l}}{dt} + \mu\frac{d\mathbf{l}}{dt} = -\frac{\delta E}{\delta\mathbf{l}}, \tag{5}$$

where λ is the orbital inertia density, μ the Cross-Anderson [8] orbital viscosity, and $-\delta E/\delta\mathbf{l}$ at constant

 0031-9007/96/77(25)/5086(4)$10.00

phase the driving torque acting on $\mathbf{l}$; the calculation shows that $d_\parallel$ and $d_\perp - 1$ are determined by μ and λ, respectively. Thus

$$d_\parallel = \frac{\gamma}{2\pi}\,\frac{m\mu}{\hbar\rho_{s\perp}}, \tag{6}$$

$$1 - d_\perp = 2m\lambda/\hbar\rho_{s\perp}, \tag{7}$$

where the texture-dependent dimensionless number γ is given by an integral over a unit cell of the vortex lattice in the plane perpendicular to the rotation axis,

$$\gamma = \int dS \sum_i (\partial l_i/\partial x)^2. \tag{8}$$

Writing γ as a scalar assumes that the properties of the vortex array are isotropic so that the integral is independent of the direction of x in this plane.

Since our experimental method for measuring mutual friction has been reported elsewhere [9], and results for the B phase have been given in [10], we give only a brief description here. The ^{3}He is contained in two disc shaped regions of diameter 4 cm and height 100 μm, separated by a circular aluminized kapton diaphragm. Vortex lines perpendicular to the diaphragm are generated by rotation of the cryostat, and superfluid flow perpendicular to these is produced by electrostatic excitation of the normal modes of transverse vibration of the diaphragm using electrodes in the roof of the cell. The coefficients α and α' are measured through their effect on the two near-degenerate ($\Delta\nu/\nu = 0.032$) modes with single nodal lines along mutually perpendicular cell diameters. The dissipative term in the mutual friction causes an increase $2\alpha\Omega$ in the bandwidth of each mode, and the reactive term and the Coriolis force together produce a net coupling proportional to $\alpha' - 1$ between the two orthogonal components. We thus measure directly the quantities that appear in Eqs. (3) and (4).

Figure 1 shows values of α and $\alpha' - 1$ obtained for the A phase at 29.3 bars with B phase values at lower temperatures for comparison. At the $B \rightarrow A$ transition α increases discontinuously, whereas $\alpha' - 1$ jumps to a value indistinguishable from zero. The increased scatter of the α values in the A phase probably indicates that history-dependent textural effects were not completely eliminated by our procedure of cooling through T_C while rotating. The resonances were too broad for $T > 0.9T_C$ to obtain meaningful values of $\alpha' - 1$.

If we take $\rho_{s\perp}/2m$ as an estimate of the Cooper pair density and $1 - \alpha' \ll \alpha$, then the orbital inertia per Cooper pair in units of $\hbar$, estimated from Eqs. (4) and (7), is

$$\frac{2m\lambda}{\hbar\rho_{s\perp}} = (1 - d_\perp) \simeq \frac{1 - \alpha'}{\alpha^2}. \tag{9}$$

From Fig. 1 we deduce that $\alpha^2 > 16$ and hence that the orbital inertia corresponds to less than $0.005\hbar$ per

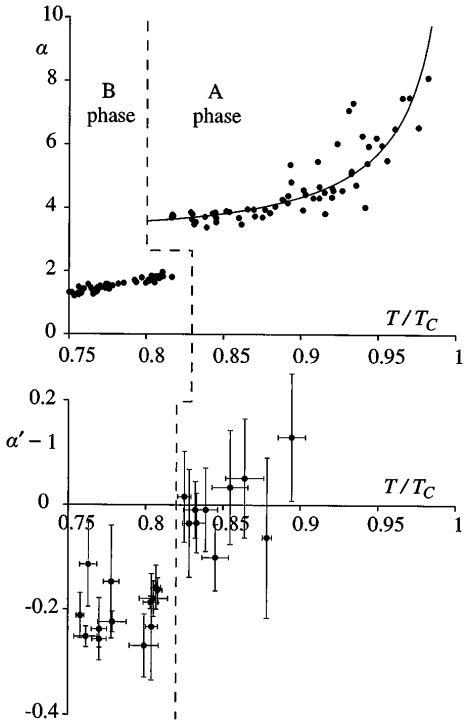

FIG. 1. Measured values of α and $\alpha' - 1$ at 29.3 bars. Data to the left of the dashed line are for the B phase, those to the right are for the A phase. The continuous curve is obtained from Eq. (10) as described in the text.

Cooper pair. This is sufficient to exclude the suggestion $\lambda = \hbar(2C - C_0)/2m$ [3].

In the limit $1 - \alpha' \rightarrow 0$, Eqs. (3) and (6) give

$$\alpha = \frac{1}{d_\parallel} = \frac{2\pi}{\gamma}\,\frac{\hbar\rho_{s\perp}}{m\mu}, \tag{10}$$

and this has been used to draw the continuous theoretical curve on Fig. 1 for $\gamma = 12.8$, $\mu = 5.8 \times 10^{-7}(1 - T/T_C)^{3/2}$ N s m^{-2} [4], and theoretical values for $\rho_{s\perp}$.

To calculate a theoretical value of γ we assume that, in our thin slab geometry, continuous doubly quantized vortices of the Anderson-Toulouse (AT) type [11] are created by rotation. To justify this assumption we note that a continuous vortex texture must terminate in appropriate point singularities (boojums) on a surface perpendicular to the axis of rotation; a boojum can be thought of as an AT vortex whose radial length scale diminishes to zero at the surface. Since at our highest speed of rotation two-quantum vortices are about 300 μm apart in a volume only 100 μm high, we expect the texture in each vortex to be hardly affected by the proximity of others, because its radial scale will be set by the cell height. Only at higher vortex density (or greater cell height) would we expect the vortex textures to merge to give the lattice of single quantum Mermin-Ho vortices [12] that is expected to have the lowest energy in a bulk geometry. Textures for the three possible types of AT vortex, radial (or v), circular (or w), and hyperbolic, are shown in Fig. 2 for anticlockwise

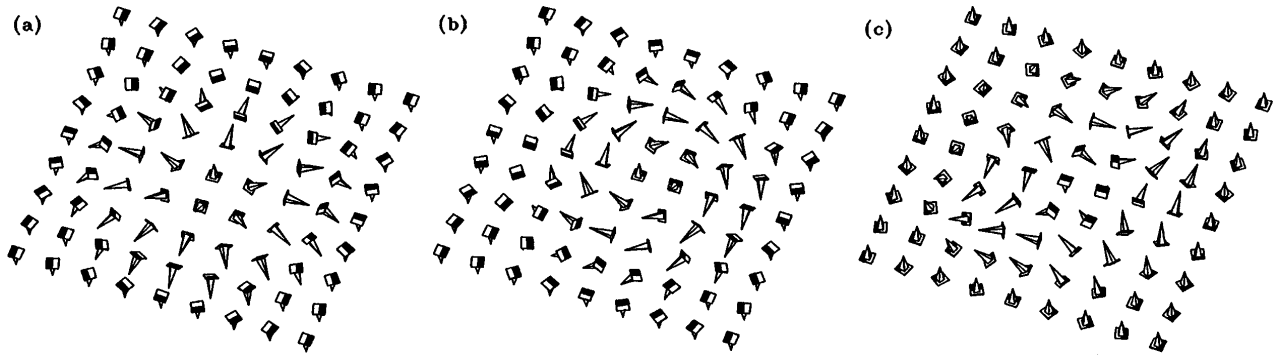

FIG. 2. Orbital texture for (a) radial, (b) circular, and (c) hyperbolic AT vortices appropriate for anticlockwise rotation. The markings on the base of the cones enable rotation of the orbital triad about **l** to be followed.

circulation. The cone symbols indicate the direction of **l**, with the black and white markings on the base enabling rotations of the orbital triad about **l** to be followed. In all cases the cones rotate two turns in a left-handed sense as the perimeter is traversed anticlockwise, corresponding to two quanta of anticlockwise circulation. For future reference note that radial, circular, and hyperbolic AT vortices appropriate to anticlockwise rotation embed in **l**-down, **l**-down, and **l**-up textures, respectively. Vortices appropriate to clockwise rotation are obtained by reversing the **l** direction.

Using Eq. (9) we calculate values for γ of 16.1, 15.8, and 15.5 for radial, circular, and hyperbolic vortices of infinite extent along the vortex axis; $T \rightarrow T_C$ values of the free energy bending coefficients were used in this calculation. Our experimental measurements cannot therefore distinguish between the different types; the agreement with the experimental value is reasonable because of possible error in the value used for the orbital viscosity and the failure of the theoretical calculation to take into account variation of vortex texture along the rotation axis.

Textural memory effects were investigated by exploiting the observation that, for any texture other than uniform **l** perpendicular to the slab, ac flow exerts a torque on **l** and hence causes dissipation by orbital viscosity, essentially the same mechanism as that which produces the mutual friction. Figure 3 shows a series of measurements of resonance bandwidth in the nonrotating state, separated by periods of rotation. The low initial dissipation (indicating a texture of good uniformity) was obtained by cooling through T_C while rotating in a positive (earthwise) sense at 0.42 s^{-1} and then stopping rotation. Measurements connected by solid and dashed lines are separated by periods of positive and negative rotation, respectively. The two unconnected points were separated by a 19-hour wait without rotation. It is clear that rotation in the initial sense tends to reduce dissipation in the nonrotating state, and rotation in the opposite sense to increase it. The system thus remembers its initial sense of rotation, and rotation in the "wrong" sense produces a less uniform nonrotating texture. Rotation in the "right" sense can eventually reduce dissipation below the initial level. The roles of positive and negative rotations can be reversed by a sufficient number of successive rotations in the wrong direction; the nonrotating bandwidth achieves a maximum value of about 0.58 Hz during this training process and about ten further rotations are needed to reduce the bandwidth to that expected for a good texture. These observations show that ^{3}He-*A* exists in two different states of low dissipation, which we identify as **l**-up and **l**-down textures. Further evidence that our lowest dissipation textures correspond to uniform **l** is provided by the $>8\%$ decrease in resonant frequency on cooling into the *B* phase, showing that $\rho_{s\perp}$ is the effective superfluid density in the *A* phase.

The textural memory effect is explained by noting that cooling through T_C while rotating should produce the vortices of minimum energy (we believe these to be the circular AT vortex). On stopping rotation the vortices are swept out leaving behind a uniform **l** texture in the appropriate direction for the type of vortex and sense of rotation. Further rotation in the same sense should again embed minimum energy vortices in this uniform texture, but to achieve rotation in the opposite sense we have either to insert vortices of an energetically unfavorable type or invert the bulk **l** texture; it is likely that both processes occur. We then expect a nonrotating texture of

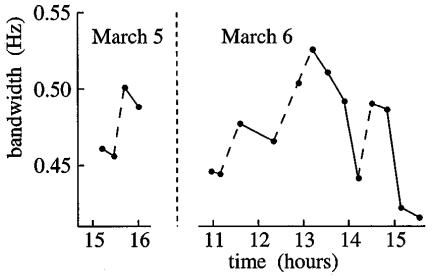

FIG. 3. Measurements of nonrotating bandwidth, separated by periods of positive (continuous lines) and negative (dashed lines) rotation after cooling through T_C with positive rotation.

higher dissipation associated with domain walls between **l**-up and **l**-down regions, until after repeated periods of rotation in the new sense the **l** texture is entirely inverted.

We observed a linear decrease of resonant frequency with rotation rate when a uniform texture is rotated in the right sense, which provides evidence that the vortex textures are as envisaged above. Since the frequency is proportional to the effective value of $\sqrt{\rho_s}$ a texture that gave an isotropic average of the ρ_s tensor would reduce the frequency by a factor $\sqrt{5/6}$, a reduction of 8.7%. If we assume that the effective value of $\sqrt{\rho_s}$ for the vortex texture is determined by an isotropic average within a radius r around each vortex and by $\rho_{s\perp}$ elsewhere, then the observed fractional reduction in resonant frequency of 3.5 Ω % is obtained for $r = 92$ μm, independent of angular velocity. This length is of the order of the sample height as expected for well separated AT vortices. The frequency reduction, like the dissipation, is significantly larger for rotation in the wrong sense; it is not clear how far this is associated with a different vortex type and how far with the presence of domain walls between **l**-up and **l**-down regions.

Cooling through T_C not rotating but still in a compensated magnetic field produces a texture different from those discussed above. The initial nonrotating bandwidth is only slightly greater than that of the uniform texture (typically by 0.05 Hz), but the first rotation in any direction increases the nonrotating bandwidth to a value ($\sim$0.8 Hz) substantially higher than that reached during the inversion of the bulk **l** texture by the training process discussed above. A much smaller change in frequency between rotating and nonrotating states is observed after this process, showing that the nonrotating texture is highly distorted. Training of this very distorted texture by repeated rotations in the same direction does, however, eventually produce a uniform nonrotating texture. We propose that the small increase in initial bandwidth is due to domain walls between regions of **l**-up and **l**-down formed during the cooling process and suggest that the first rotation causes the domain walls to become decorated with single quantum vortices and stretched to form vortex sheets in the way envisaged by Parts *et al.* [13]. Note that a domain wall, whether decorated with vortices or not, becomes a line singularity at the surface, in the same way that an AT vortex becomes a point singularity (boojum). The large residual dissipation after the first rotation is stopped suggests that a domain wall which has been elongated in this way does not readily shorten when vorticity is removed, perhaps because of pinning. The difference between this behavior and that observed when the **l** texture is inverted by repeated rotations in the wrong sense is perhaps explained by assuming that dipole-unlocked domain walls are produced on cooling through T_C without rotation, whereas inversion of **l** below T_C proceeds via dipole-locked domain walls.

The experiments reported here have thus established three basic properties ^{3}He-*A*: negligible orbital inertia; dissipation by orbital viscosity; association of **l**-up and **l**-down textures with opposite directions of rotation.

This work was supported by EPSRC through Research Grant No. GR/K59835 and by the award of research studentships to T. D. C. B. and J. B. C.

*Present address: Physics Department, University of Jyväskylä, P.O. Box 35, 40351 Jyväskylä, Finland.

[1] Ü. Parts, J. M. Karimäki, J. H. Koivuniemi, M. Krusius, V. M. H. Ruutu, E. V. Thuneberg, and G. E. Volovik, Phys. Rev. Lett. **75**, 3320 (1995).

[2] E. B. Sonin, Rev. Mod. Phys. **59**, 87 (1987).

[3] See, for example, the Comment by M. Liu, Phys. Rev. Lett. **55**, 441 (1985), and the Reply to it by H. E. Hall, Phys. Rev. Lett. **55**, 442 (1985), and references therein.

[4] J. C. Wheatley, in *Progress in Low Temperature Physics*, edited by D. F. Brewer (North-Holland, Amsterdam, 1978), Vol. VIIa, p. 1.

[5] See W. F. Brinkman and M. C. Cross, in *Progress in Low Temperature Physics* (Ref. [4]), Vol. VIIa, p. 105, and references therein.

[6] J. R. Hook, A. D. Eastop, E. Faraj, S. G. Gould, and H. E. Hall, Phys. Rev. Lett. **57**, 1749 (1986).

[7] R. J. Donnelly, *Quantized Vortices in Helium II* (Cambridge University Press, Cambridge, England, 1991), p. 89.

[8] M. C. Cross and P. W. Anderson, in *Proceedings of the 14th International Conference on Low Temperature Physics* (North-Holland, Amsterdam, 1975), Vol. 1, p. 29.

[9] J. R. Hook, T. D. C. Bevan, A. J. Manninen, J. B. Cook, A. J. Armstrong, and H. E. Hall, Physica (Amsterdam) **210B**, 251 (1995).

[10] T. D. C. Bevan, A. J. Manninen, J. B. Cook, A. J. Armstrong, J. R. Hook, and H. E. Hall, Phys. Rev. Lett. **74**, 750 (1995); **74**, 3092(E) (1995).

[11] V. R. Chechetkin, Zh. Eksp. Teor. Fiz. **71**, 1463 (1976) [Soviet Phys.—JETP **44**, 766 (1976)]; P. W. Anderson and G. Toulouse, Phys. Rev. Lett. **38**, 508 (1977).

[12] T. Fujita, M. Nakahara, T. Ohmi, and T. Tsuneto, Prog. Theor. Phys. **60**, 671 (1978).

[13] Ü Parts, E. V. Thuneberg, G. E. Volovik, J. H. Koivuniemi, V. M. H. Ruutu, M. Heinilä, J. M. Karimäki, and M. Krusius, Phys. Rev. Lett. **72**, 3839 (1994).